Published in final edited form as:
Am J Physiol Lung Cell Mol Physiol. 2006 January ; 290(1): L32–L40. doi:10.1152/ajplung.00133.2005.

Transgenic extracellular superoxide dismutase protects postnatal alveolar epithelial proliferation and development during hyperoxia

Richard L. Auten[1,2], **Michael A. O'Reilly**[3,4], **Tim D. Oury**[5], **Eva Nozik-Grayck**[1], and **Mary H. Whorton**[1]

1*Neonatal-Perinatal Research Institute, Department of Pediatrics, Duke University Medical Center, Durham, North Carolina*

2*Neonatal-Perinatal Research Institute, Department of Cell Biology, Duke University Medical Center, Durham, North Carolina*

3*Department of Pediatrics, University of Rochester, Rochester, New York*

4*Department of Environmental Medicine, University of Rochester, Rochester, New York*

5*Department of Pathology, University of Pittsburgh, Pittsburgh, Pennsylvania*

Abstract

Transgenic (TG) human (h) extracellular superoxide dismutase (EC-SOD) targeted to type II cells protects postnatal newborn mouse lung development against hyperoxia by unknown mechanisms. Because alveolar development depends on timely proliferation of type II epithelium and differentiation to type I epithelium, we measured proliferation in bronchiolar and alveolar (surfactant protein C-positive) epithelium in air and 95% O_2-exposed wild-type (WT) and TG hEC-SOD newborn mice at postnatal *days 3*, *5*, and *7* (P3–P7), traversing the transition from saccular to alveolar stages. We found that TG hEC-SOD ameliorated the 95% O_2-impaired bromodeoxyuridine uptake in alveolar and bronchiolar epithelium at P3, but not at P5 and P7, when overall epithelial proliferation rates were lower in air-exposed WT mice. Mouse EC-, CuZn-, and Mn-SOD expression were unaffected by hyperoxia or genotype. TG mice had less DNA damage than 95% O_2-exposed WT mice at P3, measured by TdT-mediated dUTP nick end labeling ($P < 0.05$). Hyperoxia induced cell-cycle inhibitory protein $p21^{cip/waf}$ mRNA at P3, WT > TG, $P = 0.06$. 95% O_2 impaired apical expression of type I cell protein (T1α) in WT but not in TG mice at P3 and increased T1α in WT and TG mice at P7. Reducing the 95% O^2-induced impairment of epithelial proliferation at a critical window of lung development was associated with protection against DNA damage and preservation of apical T1α expression at P3.

Keywords

type I cell; T1α; deoxyribonucleic acid damage

EXTRACELLULAR SUPEROXIDE DISMUTASE(EC-SOD) is predominantly found in extracellular matrix of adult animals (9). In newborns, it is also expressed intracellularly in lung epithelium (13,22). It is the most abundant SOD isoform in the lung, and it may regulate signaling pathways mediated by reactive oxygen species in the developing lung (9). For example, EC-SOD expression has been shown to govern the bioavailability of nitric oxide (27), an important signaling pathway in early and late lung development (33,36).

Address for reprint requests and other correspondence: R. L. Auten, DUMC Box 3373, Durham, NC 27710 (e-mail: auten@duke.edu).

We previously showed that transgenic (TG) overexpression of human (h) EC-SOD preserved lung development in newborn mice exposed to 21 days of hyperoxia (1). The mechanisms of this protection are unknown but may include preservation of epithelial proliferation, particularly in type II pneumocytes, which are progenitor cells for type I epithelial cells that develop after the transition from saccular to alveolar stages of lung development (26).

In rodents, extreme hyperoxia impairs overall pulmonary epithelial proliferation in the immediate postnatal period (4,35). Likewise, in the baboon model of clinical bronchopulmonary dysplasia (BPD), alveolar epithelial proliferation is initially impaired, followed by hyperplasia of type II alveolar epithelial cells, which do not form normal alveoli (19). Because impaired type II cell proliferation and alveolar differentiation is a hallmark of BPD, we hypothesized that targeting EC-SOD to type II cells would protect the lung from oxidative damage and preserve orderly type II cell proliferation.

MATERIALS AND METHODS

Reagents

Secondary antibodies and detection reagents were from Vector (Burlingame, CA) except where otherwise noted. Other reagents were from Sigma (St. Louis, MO) except where noted.

Hyperoxia and Air Exposures

Animal experimental procedures were approved by the Duke University Institutional Animal Care and Use Committee. The surfactant protein C (SP-C) EC-SOD TG mouse (10) and the neonatal hyperoxia exposure regimen have been previously described in detail (1). ECSOD TG heterozygotes were bred with wild-type (WT) C57BL/6 mice (>20 generations; Jackson Laboratories, Bar Harbor, ME). Newborn mice delivered spontaneously to time-mated pregnant dams were exposed to air or 95% O_2, beginning on the day of birth for up to 7 days. Nursing dams were alternated daily between air and hyperoxia-exposed litters. Litter sizes were adjusted by culling pups to maintain balanced litter size among exposure groups. At postnatal *days 3*, *5*, and *7* (P3–P7), air and hyperoxia-exposed groups were injected 6 h before harvest with bromodeoxyuridine (BrdU, 10 mg/kg) subcutaneously according to the manufacturer's directions (Zymed, South San Francisco, CA). Pups were killed with 150 mg/kg pentobarbital sodium intraperitoneally, and lungs were inflation fixed with 10% phosphate-buffered formalin at 25 cmH_2O pressure for 30 min, immersed overnight in fixative at 4°C, and then paraffin embedded and sectioned at 4–6 μm. In littermates, lungs were removed and snap frozen in liquid nitrogen for protein and RNA analysis. Genotyping was performed by PCR analysis of tail snips as described previously (1).

BrdU Uptake/Ki67 Labeling: P3–P7

BrdU histochemical staining and analysis were performed as previously described in detail (4). Four nonoverlapping randomly chosen ×400 fields from two random sections were examined by an observer masked to treatment condition. Immunolabeled nuclei in epithelial cells lining air sacs and in bronchiolar epithelial cells were counted, along with unlabeled hematoxylin-counterstained nuclei.

To evaluate cell proliferation with a second method, similar sections were immunostained with anti-Ki67 (Novacastra, Norwell, MA). Ki67 is a nonhistone chromosomal protein that is expressed during active cell cycling, but not in response to DNA damage. After dewaxing and rehydrating, sections were treated with microwaving for 20 min in 0.01 M sodium citrate. Sections were then peroxidase quenched in 0.3% hydrogen peroxide (H_2C_2) in methanol, blocked 1 h in 5% horse serum in PBS, pH 7.4, treated sequentially with avidin and biotin according to the manufacturer's directions (Vector), and then incubated overnight at 4°C with

1:50 anti-Ki67 in 0.1% PBS-Tween 20 and 2% horse serum. Antigen was detected with secondary horse anti-mouse:biotin followed by ABC Elite, diaminobenzidine (DAB), according to the manufacturer's directions, and counterstaining with hematoxylin. Labeling indexes were calculated in alveolar (cells lining the distal air sacs and alveoli) and bronchiolar epithelial cells for both BrdU and Ki67 in each treatment group (n = 5–6/group).

BrdU/SP-C Colocalization: P3

We examined the proliferation of alveolar type II epithelium, the progenitor cells of alveolar type I epithelium at P3, because this was the time at which hyperoxia had the greatest effect on alveolar epithelial proliferation (20). Sections from P3 air- and hyperoxia-exposed BrdU-injected pups, WT and TG, were first immunostained with rabbit anti-mouse pro-SP-C (Santa Cruz Biotechnology) followed, in the same tissue sections, by staining with anti-BrdU. Briefly, dewaxed and rehydrated sections were boiled in antigen unmasking buffer (Vector) for 10 min and cooled. Tissue sections were then probed with a polyclonal goat anti-pro-SP-C 1:200, followed by biotinylated horse anti-goat detected with ABC Elite, as above, and visualized with DAB. These sections were then incubated at room temperature with 4 N HCl for 9 min, washed for 10 min three times with PBS 0.1% Tween (PBS-T), quenched in H_2O_2 for peroxidases as above, rinsed in PBS-T, and then blocked in 5% BSA in PBS for 1 h. Sections were then blocked in avidin-biotin, as above, and incubated with ABC Elite. The BrdU signal was detected with the peroxidase substrate VIP (Vector), which yields a purple color to distinguish its signal from the SP-C DAB signal. Sections were examined under oil immersion. A minimum of 500 SP-C-positive cells per animal were counted using five animals per treatment group. BrdU labeling index = number of BrdU/SP-C colocalizing cells ÷ total number of SP-C-positive cells.

EC-SOD Western Blotting at P3

Maximal effects on proliferation were observed at P3; therefore, we measured native mouse and TG hEC-SOD expression at P3. Lungs from four WT and four EC-SOD TG mice in air and 95% O_2 treatment groups at P3 were homogenized, and protein extracts, 20 μg/lane, were analyzed on polyacrylamide gels (15% ReadyGel; Bio-Rad, Hercules, CA) with molecular size markers and electroblotted onto polyvinylidene fluoride membrane (ECL; Amersham, Piscataway, NJ). hEC-SOD was detected with rabbit anti-human EC-SOD 1:5,000 (1), followed by goat anti-rabbit peroxidase 1:10,000, and then detection by enhanced chemiluminescence (Amersham) and exposure to film (Hyperfilm, Amersham). Blots were stripped (Restore; Pierce, Rockford, IL) and reprobed with rabbit anti-mouse EC-SOD and detected as above and as previously described (1). Relative abundance of each isoform was analyzed from scanned fluorograms using ImageQuant 5.0 (Molecular Dynamics, Piscataway, NJ). Total pixels above background within a rectangle placed around each band were quantified and compared.

Mn-SOD and CuZn-SOD Western Blotting at P3

To ensure that SOD effects were specific to the EC-SOD isoform, we measured Mn-SOD and CuZn-SOD on immunoblots prepared as above. Four or five animals per treatment group were analyzed. Blots were detected with mouse monoclonal anti-Mn-SOD (BD Biosciences) 1:10,000 or rabbit anti-rat (mouse reactive) CuZn-SOD (Research Diagnostics) 0.25 pg/ml, followed by goat anti-mouse: peroxidase conjugate 1:30,000 in PBS plus 0.1% Tween and 5% BSA and detected as above. Blots were stripped (Restore) and redetected with 30 ng/ml polyclonal rabbit anti-β-actin (Abcam, Cambridge, MA) to control for loading and transfer.

EC-SOD Immunohistochemistry at P3

To determine the cellular localization of mouse and hEC-SOD expression in WT and TG newborn mice in this model system, we detected both human and mouse EC-SOD in paraffin sections from all treatment groups with species-specific antibodies previously described (1, 10). Sections were incubated with anti-mouse EC-SOD or anti-human EC-SOD and detected with biotinylated secondary antibodies followed by ABC Elite and DAB chromagen, as described.

EC-SOD mRNA at P3

To measure the effects of air or 95% O_2 exposure on native mouse EC-SOD mRNA transcription and SP-C promoter-driven TG hEC-SOD mRNA transcription, or on housekeeping gene glyceraldehyde-3-phosphate dehydrogenase (GAPDH) mRNA transcription in newborn mouse lung at 3 days, total RNA was extracted from flash-frozen lungs of WT and TG mice in four animals per treatment group, air vs. hyperoxia, WT vs. TG according to the manufacturer's directions (TRIzol, Invitrogen). Quantitative real-time RT-PCR was performed on 0.5-μg samples.

Mouse EC-SOD primers: forward-TTCTTGTTCTACGGCTTGCTAC, reverse-CTCCATCCAGATCTCCAGCACT. Human EC-SOD primers: forward-AGACACCTTCCACTCTGAGG, reverse-GTTTCGGTACAAATGGAGGC. Mouse GAPDH primers: forward-TTCTTACTCCTTGGAGGCCATG, reverse-CATCTTGGGCTACACTGAGGAC.

RNA was reverse transcribed in capillary tubes according to the manufacturer's directions (LightCycler RNA Amplification, SYBR Green I; Roche, Indianapolis, IN) using primer concentrations of 0.5 μM in the reaction at 55°C for 10 min (20°C/s slope), followed by a denaturing step of 95°C for 30 s. PCR was carried out in the LightCycler (Roche) for 50 cycles of denaturing: 95°C, no hold time (20°C/s), annealing: 57° for 10 s (20°C/s), and extension: 72°C for 13 s (2°C/s).

The amplicon signals for mouse EC-SOD and hEC-SOD at the crossing points indicating linear amplification of PCR products were compared after normalizing to GAPDH crossing point signal as we have previously described (28).

TdT-Mediated dUTP Nick End Labeling: P3

Sections from all treatment groups at P3 were dewaxed, rehydrated, and incubated in 10 μg/ml proteinase K at 37°C for 15 min, rinsed in PBS, then incubated in terminal transferase labeling mixture containing fluorescein-conjugated dUTP for 30 min at 37°C, according to the manufacturer's directions (In Situ Death Detection, Roche). Maximum signal (positive control) was achieved by pretreating sections with DNase I before TdT-mediated dUTP nick end labeling (TUNEL). Negative controls were sections incubated without terminal transferase. Sections were counterstained with 4′,6-diamidino-2-phenylindole (DAPI) as described previously (5). TUNEL and DAPI images (2 pair/section) were captured from two random sections from four animals per treatment group at ×200 as noted above, using appropriate filters and identical exposure conditions. Paired images were quantified using Metamorph software. TUNEL signal in each captured field (pixels above background) was normalized to total nuclear number in each field, represented by the DAPI signal, as we described previously (5).

$p21^{cip/waf}$, p53 RNase Protection Assay: P3

Total lung RNA from eight WT and TG pups per treatment condition at P3 was hybridized according to our previously described methods to [^{32}P]UTP-labeled cRNA probes for $p21^{cip/waf}$ and p53, inhibitors of cell-cycle progression both induced by hyperoxic-DNA

damage (23). cRNA probes for GAPDH were included for normalization, and each protected p53 and $p21^{cip/waf}$ mRNA signal obtained from exposure of gels to a phosphor storage screen was analyzed using ImageQuant as above. Each signal was normalized to the corresponding GAPDH signal in the same lane. Results were compared with the mean normalized signal for air-exposed WT controls at 3 days.

Type I Cell α Protein Western Blotting: P3, P7

Total lung protein (20 μg/lane) from four animals per genotype per treatment group were analyzed by Western blot as noted previously. Blots were detected with anti-type I cell α protein (T1α) 1:20,000 and goat anti-hamster peroxidase 1:20,000 using ECL and film (CL-Xposure, Pierce). Blots were stripped (Restore) and redetected with polyclonal anti-β-actin (Abcam) at 1:20,000 to verify equal loading and transfer. Film images were quantified using ImageQuant as noted above to compare T1α abundance in whole lung.

T1α Immunohistochemistry: P3, P7

Random sections were chosen from four animals in each treatment group as above. Sections were incubated without antigen retrieval with hamster anti-mouse monoclonal anti-T1α (8) (clone 8.1.1, Univ. of Iowa Hybridoma Bank) at 1:1,000, followed by anti-hamster peroxidase and tyramide signal amplification using tyramide-biotin (Molecular Probes) followed by avidin-peroxidase 1:1,000 (Vector) and DAB, counterstaining with hematoxylin.

Statistical Analysis

Between-group differences were analyzed by ANOVA and post hoc comparisons used Tukey-Kramer. Data were analyzed using statistical analysis software (JMP; SAS, Cary, NC). Significant differences were accepted at $P < 0.05$, assuming the use of an α error = 0.05 and a β error = 0.10.

RESULTS

Alveolar and Bronchiolar Epithelial Proliferation: P3–P7

Hyperoxia markedly impaired both bronchiolar and alveolar epithelial proliferation at P3 and P5, as measured by BrdU uptake or Ki67 labeling (Fig. 1). Alveolar and bronchiolar epithelial proliferation was significantly preserved in P3 mice overexpressing hEC-SOD during 95% O_2 exposure. Alveolar epithelial proliferation was also slightly higher in air-exposed TG mice. By P5 and P7, the hyperoxia-induced decrement in-alveolar and bronchiolar epithelial proliferation labeling indexes had narrowed. BrdU uptake at P7 was statistically lower in alveolar epithelium in 95% O_2-exposed TG mice, but the magnitude of difference was small compared with differences at P3 (Fig. 1).

Type II Alveolar Proliferation at P3

Hyperoxia-induced disruption of proliferation, detected by BrdU uptake and Ki67 labeling, and its prevention by EC-SOD overexpression were maximal at P3; therefore, the remaining studies were predominantly focused on effects at P3. We studied effects of hyperoxia and EC-SOD overexpression on type II cells since they are susceptible to hyperoxia and are the progenitor cells for type I alveolar epithelium (26). As shown in Fig. 1, 95% O_2 significantly impaired type II (pro-SP-C-positive) proliferation at P3, but TG EC-SOD overexpression significantly protected type II cells from this effect.

Effects of Hyperoxia at P3 on Postnatal EC-SOD Expression

Western blotting—To determine whether alterations in EC-SOD protein expression contributed to the protective effects in TG mice exposed to hyperoxia, we examined both mouse

and hEC-SOD expression at P3 in air- and 95% O_2-exposed mice. On immunoblots, we found that 95% O_2 had no significant effects on either mouse or hEC-SOD expression at P3 (Fig. 2). There were no apparent effects on EC-SOD processing or proteolytic cleavage, since the relative abundance of each EC-SOD isoform at ~34 kDa remained similar in air and 95% O_2.

Effects of Hyperoxia at P3 on Mn- and CuZn-SOD Expression

Western blotting—To determine whether hyperoxia exposure or genotype had affected Mn- or CuZn-SOD protein expression, immunoblots from air- and 95% O_2-exposed WT and TG groups were probed for both Mn- and CuZn-SOD (Fig. 2). We saw no effect of hyperoxia or genotype on Mn- or CuZn-SOD accumulation in whole lung homogenates at P3.

Real-Time PCR

Because hyperoxia can induce SP-C transcription (2) and the SP-C promoter drives the hEC-SOD expression (10), we measured the effect of hyperoxia on mouse and hEC-SOD mRNA by quantitative real-time RT-PCR and found that mouse EC-SOD mRNA normalized to GAPDH mRNA was unaffected by genotype or 95% O_2 exposure at P3. hEC-SOD mRNA was detected only in the TG mice and was not increased by 95% O_2 at P3 (Fig. 2).

Immunohistochemistry

Mouse EC-SOD was observed predominantly in bronchiolar epithelium (Fig. 2), and weak staining was evident in vascular smooth muscle (not shown). We did not detect EC-SOD in pulmonary endothelial cells. hEC-SOD expression was confined to bronchiolar and alveolar epithelium in TG mice, as we have previously noted, but was exclusively cytoplasmic at the time points examined (Fig. 2) (1). Hyperoxia had no apparent effect on the cellular distribution of either mouse EC-SOD or hEC-SOD expression.

$p21^{cip/waf}$ and p53 Expression

RNase protection—We found that 95% O_2 induced $p21^{cip/waf}$ mRNA accumulation (normalized to GAPDH mRNA) in whole lung from both WT and TG mice, with a trend toward reduced p21 induction in TG mice ($P < 0.06$ vs. WT; Fig. 3). We did not observe any increase in p53 mRNA or any effect on L32 cyclin, another “housekeeping” mRNA (data not shown).

DNA Nicking (TUNEL) at P3

DNA damage induced by hyperoxia may contribute to impaired proliferation by halting cell cycling to allow repair (23). To screen for DNA damage, we performed TUNEL in situ. Terminal transferase labeling identifies nicked DNA, due to necrosis, apoptosis, and mitosis, so not all TUNEL staining indicates DNA damage. We found that 95% O_2 exposure induced TUNEL in bronchiolar and alveolar epithelium as previously described (5,21) (Fig. 4). TUNEL was decreased in hyperoxia-exposed TG mice.

T1α Western Blotting

Hyperoxia had no consistent effect on whole lung T1α expression at P3, regardless of genotype. As shown in Fig. 5, expression was variable in both WT and TG mice regardless of exposure at P3. In contrast, hyperoxia induced whole lung T1α expression at P7 in both WT and TG animals. β-Actin expression was similar among all treatment groups.

T1α Immunohistochemistry

In contrast to the inconsistent effect of hyperoxia on whole lung T1α at P3, hyperoxia uniformly impaired apical but not interstitial expression of T1α in WT but not TG mice at P3 (Fig. 6). At

P7, T1α was consistently expressed on the apical surfaces of alveolar epithelium, in both WT and TG mice, and there was no obvious effect of hyperoxia on subcellular expression.

DISCUSSION

Hyperoxia exposure in newborn mice, 95% O_2 × 7 days beginning at birth, then 60% O_2 × 14 days, impairs alveolar formation, measured as depressed alveolar surface density and volume density at P21. This was prevented in hEC-SOD TG mice (1). The present studies were undertaken to elucidate the mechanisms by which hEC-SOD overexpression preserves lung development. We found that 95% O_2 exposure profoundly impairs alveolar and bronchiolar epithelial proliferation at P3, measured by either BrdU uptake or Ki67 expression, when lung development begins the transition between saccular and alveolar phases in the mouse. Hyperoxia-impaired epithelial proliferation persisted at P5 and P7, although the magnitude of impairment was diminished. TG hEC-SOD overexpression in alveolar and, to a lesser extent, bronchiolar epithelium significantly preserved alveolar and bronchiolar epithelial proliferation at P3 in pups exposed to hyperoxia.

We found that the labeling indexes for BrdU uptake and Ki67 showed parallel trends, although the absolute values were not identical. At P7, for example, BrdU uptake in alveolar epithelium was actually lower in 95% O_2-exposed TG mice than in WT littermates, but there were no such differences in Ki67 labeling. In contrast, we found that air-exposed TG mice demonstrated more BrdU uptake in alveolar epithelial cells than air-exposed WT mice, but no differences in Ki67 were observed. We do not know whether this difference in proliferation is maladaptive, and no overt differences in lung morphology have been reported in EC-SOD TG adult mice (10), although this has not been studied in detail.

Ki67 is expressed in cycling cells, maximally expressed during M-phase, whereas BrdU uptake may occur during DNA repair in DNA-damaged, non-cycling cells (6,16), which would be expected during hyperoxia (23). Ki67 and BrdU may therefore not identify identical cell populations, with Ki67 being the more specific marker of proliferation.

We attribute these observed effects to TG hEC-SOD (15). Native mouse EC-SOD expression in newborns, in whole lung or by immunohistochemistry, was unaffected by 95% O_2 exposure or by genotype at P3. Mouse EC-SOD expression was restricted to alveolar and bronchiolar epithelium and vascular smooth muscle. Extracellular expression was less widespread than intracellular expression in the newborn mouse, as previously described in newborn rabbits and rats (13,17,22). TG hEC-SOD expression was overwhelmingly intracellular, and this was unaffected by hyperoxia. We did not measure activity levels of antioxidant enzymes in lungs of neonatal mice at P3, but we previously reported that EC-SOD activity in TG neonatal mice at P7 was ~2.5-fold the activity observed in WT mice (1). TG hEC-SOD did not affect native antioxidant enzyme expression or activity in adult hyperoxiaexposed mice (10).

There were no effects of hyperoxia or genotype on the other SOD isoforms, CuZn-SOD or Mn-SOD, determined by Western blotting. Hyperoxia has previously been reported to induce some antioxidant systems in newborns, both premature and term newborns (12), but this is species specific with relatively modest increases in total SOD activity (<20%) observed in 2-day-old mice exposed to 95% O_2 (11).

The differences in the protective effects of hEC-SOD over-expression on proliferation (alveolar > bronchiolar) may be due to the relatively greater expression of hSP-C promoterdriven hEC-SOD expression in type II cells. Because we found mouse EC-SOD expressed at relatively high levels in bronchiolar epithelium at P3, there may be less additional EC-SOD activity conferred by TG hEC-SOD, although this was not directly tested.

The relationship of oxidative stress to cellular proliferation during lung development is complex. Survival after hyperoxia in in vitro and in vivo models requires the arrest of cell cycling to permit repair of hyperoxia-induced DNA damage, which is associated with induction of the cyclin-dependent kinase inhibitor $p21^{cip/waf}$ (23). DNA nicking (TUNEL) was induced in hyperoxia-exposed WT animals, but not in EC-SOD TG animals at P3. Although TUNEL may also identify dividing and apoptotic cells, we previously found that hyperoxia-induced TUNEL in newborn lung seldom identified apoptotic cells (5). We found that hyperoxia increased $p21^{cip/waf}$ mRNA in whole lung from WT animals at P3, which displayed the most significant proliferation arrest. This increase was partly prevented in EC-SOD TG animals at P3. Hyperoxia did not induce p53 mRNA, as was expected, since its effects on p53 are mediated predominantly through protein stability rather than transcription (14,24). Effects on $p21^{cip/waf}$ and p53 mRNA at the whole lung level are limited by the choice(s) of reference mRNAs that might themselves be affected. In our studies, there was little variation in GAPDH (or L32 cyclin, data not shown) mRNA signal. Because we studied mRNA in whole lung, we were unable to determine cell specificity of effects on $p21^{cip/waf}$ expression. Proliferation arrest at a critical period of lung development may impair the appropriate patterning of type II differentiation and type I cell formation during postnatal lung development.

We have previously shown that this model of hyperoxia-impaired neonatal lung development, continued to P21, ultimately leads to impaired alveolization and that this is significantly prevented in TG hEC-SOD mice (1). This led us to conclude that preservation of alveolar and bronchiolar epithelial proliferation in TG hEC-SOD mice is likely adaptive, accompanied by safe repair of hyperoxia-induced DNA damage, although we did not evaluate this directly.

Alveolar formation depends on orderly differentiation of type II → type I cells. We found that hyperoxia consistently impaired apical expression of T1α in WT mice at P3, but not TG mice (Fig. 6). T1α is normally expressed on apical surfaces of type I cells, but hyperoxia-exposed WT mice demonstrated qualitatively less apical labeling than TG mice at P3. By *day 7*, there were no apparent differences in localization. We did not observe consistent effects of hyperoxia on T1α in whole lung homogenates, in either WT or TG mice, at P3. Hyperoxia induced T1α expression in whole lung from both WT and TG mice at P7, consistent with earlier observations of T1α expression in adult mice (7).

The precise function of T1α in type I homeostasis is not known, but gene deletion leads to failure of normal alveolar formation and death from respiratory failure at birth (29). In vitro studies suggest that T1α may be necessary to maintenance of the flattened attenuated shape of the type I cell (31,32). In vitro studies show that injury to type II cells may lead to differentiation or transdifferentiation to intermediate cell types before type I cells are formed (20). Lack of apical labeling in the hyperoxia-exposed WT animals at P3 may represent this phenomenon.

EC-SOD overexpression in type II cells may also affect direct and indirect regulation of T1α expression by oxygen or reactive oxygen species. Cao and colleagues (7) have shown that hyperoxia induces increased T1α expression in adult mice through effects on nuclear transcription factors Sp1 and Sp3 binding to DNA, but the identity of the molecular interaction between oxygen, reactive oxygen species, or intermediates, and Sp1/Sp3 binding and downstream effects on the T1α promoter is unknown. Hyperoxia effects may be indirectly mediated through thyroid transcription factor-1 (34), which acts on the T1α promoter (30). The relative abundance of oxygen-containing moieties will necessarily differ in the EC-SOD TG newborn mice and will likely differ in their WT littermates since newborns of many species are better able to induce enzymatic antioxidant expression during hyperoxia than adults (3). These differences may explain the delay in the hyperoxia-induced increase of T1α in newborn WT mice. Alternatively, impaired, ectopic T1α expression during hyperoxia may be due to altered protein trafficking, which we have not directly tested.

Preservation of proliferation in alveolar epithelium from 95% O_2 impairment at P3 by type II cell-targeted hEC-SOD overexpression may partly explain the protection of alveolar development against hyperoxia that we previously reported (1). Formation of alveoli depends in part on differentiation of type II cells to type I cells as the lung enters the alveolar phase of development (20) as well as type II cell-produced paracrine and autocrine factors, such as vascular endothelial growth factor, necessary for pulmonary capillary endothelial integrity (18). The initial hyperoxia-induced arrest of type II cell proliferation, followed by a maladaptive type II cell hyperplasia that fails to yield normal alveolization, is also observed in the baboon model of BPD (25). Failure to form normal alveoli may result in part from inadequate type I cell differentiation, which, in turn, could result from redox-sensitive changes to transcription factors that control expression of type I cell-specific antigen, necessary for type I cell differentiation (34).

In summary, hEC-SOD overexpression driven by the human SP-C promoter partly preserves type II alveolar epithelial and bronchiolar epithelial proliferation during severe hyperoxic stress at P3, during the transition from the saccular to alveolar phases of normal murine lung development. This effect was accompanied by protection against DNA damage, a known target of oxidative stress, partly blocking induction of $p21^{cip/waf}$ mRNA expression. Apical T1α expression, thought to be necessary to alveolar formation, was preserved in hyperoxia-exposed EC-SOD TG mice at P3 but was impaired in WT littermates. We speculate that protection of alveolar type II cells from superoxide accumulation avoids biomolecular damage and maladaptive arrest of proliferation, protecting differentiation to type I epithelium.

ACKNOWLEDGMENTS

The authors gratefully acknowledge the technical assistance of Nick Mason, Lisa Mamo, and Rhonda Staversky. Present address of E. Nozik-Grayck: Pediatric Critical Care and Developmental Lung Biology Laboratory, University of Colorado Health Science Center, Denver, CO.

GRANTS

These studies were supported by National Heart, Lung, and Blood Institute (NHLBI) Grant HL-060721 and the Children's Miracle Network (R. L. Auten), NHLBI Grant HL-067392 (M. A. O'Reilly), NHLBI Grant HL-063700 and an American Heart Association Established Investigator Award (T. D. Oury), and NHLBI Grant HL-070088 (E. Nozik-Grayck).

REFERENCES

1. Ahmed MN, Suliman HB, Folz RJ, Nozik-Grayck E, Golson ML, Mason SN, Auten RL. Extracellular superoxide dismutase protects lung development in hyperoxia-exposed newborn mice. Am J Respir Crit Care Med 2003;167:400–405. [PubMed: 12406846]
2. Allred TF, Mercer RR, Thomas RF, Deng H, Auten RL. Brief 95% O_2 exposure effects on surfactant protein and mRNA in rat alveolar and bronchiolar epithelium. Am J Physiol Lung Cell Mol Physiol 1999;276:L999–L1009.
3. Asikainen TM, White CW. Pulmonary antioxidant defenses in the preterm newborn with respiratory distress and bronchopulmonary dysplasia in evolution: implications for antioxidant therapy. Antioxid Redox Signal 2004;6:155–167. [PubMed: 14713347]
4. Auten RL Jr, Mason SN, Tanaka DT, Welty-Wolf K, Whorton MH. Anti-neutrophil chemokine preserves alveolar development in hyperoxia-exposed newborn rats. Am J Physiol Lung Cell Mol Physiol 2001;281:L336–L344. [PubMed: 11435208]
5. Auten RL, Whorton MH, Nicholas Mason S. Blocking neutrophil influx reduces DNA damage in hyperoxia-exposed newborn rat lung. Am J Respir Cell Mol Biol 2002;26:391–397. [PubMed: 11919074]
6. Beisker W, Hittelman WN. Measurement of the kinetics of DNA repair synthesis after UV irradiation using immunochemical staining of incorporated 5-bromo-2′-deoxyuridine and flow cytometry. Exp Cell Res 1988;174:156–167. [PubMed: 3275543]

7. Cao YX, Ramirez MI, Williams MC. Enhanced binding of Sp1/Sp3 transcription factors mediates the hyperoxia-induced increased expression of the lung type I cell gene T1α. J Cell Biochem 2003;89:887–901. [PubMed: 12874823]
8. Farr A, Nelson A, Hosier S. Characterization of an antigenic determinant preferentially expressed by type I epithelial cells in the murine thymus. J Histochem Cytochem 1992;40:651–664. [PubMed: 1374092]
9. Fattman CL, Schaefer LM, Oury TD. Extracellular superoxide dismutase in biology and medicine. Free Radic Biol Med 2003;35:236–256. [PubMed: 12885586]
10. Folz RJ, Abushamaa AM, Suliman HB. Extracellular superoxide dismutase in the airways of transgenic mice reduces inflammation and attenuates lung toxicity following hyperoxia. J Clin Invest 1999;103:1055–1066. [PubMed: 10194479]
11. Frank L, Bucher JR, Roberts RJ. Oxygen toxicity in neonatal and adult animals of various species. J Appl Physiol 1978;45:699–704. [PubMed: 730565]
12. Frank, L.; Sosenko, IR. Oxidants and antioxidants: what role do they play in chronic lung disease?. In: Bland, RD.; Coalson, J., editors. Chronic Lung Disease in Early Infancy. New York: Dekker; 2000. p. 257-284.
13. Giles BL, Suliman H, Mamo LB, Piantadosi CA, Oury TD, Nozik-Grayck E. Prenatal hypoxia decreases lung extracellular superoxide dismutase expression and activity. Am J Physiol Lung Cell Mol Physiol 2002;283:L549–L554. [PubMed: 12169574]
14. Kastan MB, Onyekwere O, Sidransky D, Vogelstein B, Craig RW. Participation of p53 protein in the cellular response to DNA damage. Cancer Res 1991;51:6304–6311. [PubMed: 1933891]
15. Kinnula VL, Crapo JD. Superoxide dismutases in the lung and human lung diseases. Am J Respir Crit Care Med 2003;167:1600–1619. [PubMed: 12796054]
16. Lehtinen M, Kulomaa P, Kallioniemi OP, Paavonen J, Leinikki P. Analysis of DNA synthesis in herpes simplex virus infected cells by dual parameter flow cytometry. Arch Virol 1989;107:215–223. [PubMed: 2554855]
17. Mamo LB, Suliman HB, Giles BL, Auten RL, Piantadosi CA, Nozik-Grayck E. Discordant extracellular superoxide dismutase expression and activity in neonatal hyperoxic lung. Am J Respir Crit Care Med 2004;170:313–318. [PubMed: 15117745]
18. Maniscalco WM, Watkins RH, D'Angio CT, Ryan RM. Hyperoxic injury decreases alveolar epithelial cell expression of vascular endothelial growth factor (VEGF) in neonatal rabbit lung. Am J Respir Cell Mol Biol 1997;16:557–567. [PubMed: 9160838]
19. Maniscalco WM, Watkins RH, O'Reilly MA, Shea CP. Increased epithelial cell proliferation in very premature baboons with chronic lung disease. Am J Physiol Lung Cell Mol Physiol 2002;283:L991–L1001. [PubMed: 12376352]
20. McElroy MC, Kasper M. The use of alveolar epithelial type I cell-selective markers to investigate lung injury and repair. Eur Respir J 2004;24:664–673. [PubMed: 15459148]
21. McGrath-Morrow SA, Stahl J. Apoptosis in neonatal murine lung exposed to hyperoxia. Am J Respir Cell Mol Biol 2001;25:150–155. [PubMed: 11509323]
22. Nozik-Grayck E, Dieterle CS, Piantadosi CA, Enghild JJ, Oury TD. Secretion of extracellular superoxide dismutase in neonatal lungs. Am J Physiol Lung Cell Mol Physiol 2000;279:L977–L984. [PubMed: 11053035]
23. O'Reilly MA. DNA damage and cell cycle checkpoints in hyperoxic lung injury: braking to facilitate repair. Am J Physiol Lung Cell Mol Physiol 2001;281:L291–L305. [PubMed: 11435201]
24. O'Reilly MA, Staversky RJ, Stripp BR, Finkelstein JN. Exposure to hyperoxia induces p53 expression in mouse lung epithelium. Am J Respir Cell Mol Biol 1998;18:43–50. [PubMed: 9448044]
25. O'Reilly MA, Watkins RH, Staversky RJ, Maniscalco WM. Induced p21Cip1 in premature baboons with CLD: implications for alveolar hypoplasia. Am J Physiol Lung Cell Mol Physiol 2003;285:L964–L971. [PubMed: 12871858]
26. Otto WR. Lung epithelial stem cells. J Pathol 2002;197:527–535. [PubMed: 12115868]
27. Oury TD, Day BJ, Crapo JD. Extracellular superoxide dismutase: a regulator of nitric oxide bioavailability. Lab Invest 1996;75:617–636. [PubMed: 8941209]

28. Oury TD, Schaefer LM, Fattman CL, Choi A, Weck KE, Watkins SC. Depletion of pulmonary EC-SOD after exposure to hyperoxia. Am J Physiol Lung Cell Mol Physiol 2002;283:L777–L784. [PubMed: 12225954]
29. Ramirez MI, Millien G, Hinds A, Cao Y, Seldin DC, Williams MC. T1α, a lung type I cell differentiation gene, is required for normal lung cell proliferation and alveolus formation at birth. Dev Biol 2003;256:62–73.
30. Ramirez MI, Rishi AK, Cao YX, Williams MC. TGT3, thyroid transcription factor I, and Sp1 elements regulate transcriptional activity of the 1.3-kilobase pair promoter of T1α, a lung alveolar type I cell gene. J Biol Chem 1997;272:26285–26294. [PubMed: 9334198]
31. Schacht V, Ramirez MI, Hong YK, Hirakawa S, Feng D, Harvey N, Williams M, Dvorak AM, Dvorak HF, Oliver G, Detmar M. T1α/podoplanin deficiency disrupts normal lymphatic vasculature formation and causes lymphedema. EMBO J 2003;22:3546–3556. [PubMed: 12853470]
32. Scholl FG, Gamallo C, Vilar S, Quintanilla M. Identification of PA226 antigen as a novel cell-surface mucin-type glycoprotein that induces plasma membrane extensions and increased motility in keratinocytes. J Cell Sci 1999;112:4601–4613. [PubMed: 10574709]
33. Tang JR, Markham NE, Lin YJ, McMurtry IF, Maxey A, Kinsella JP, Abman SH. Inhaled nitric oxide attenuates pulmonary hypertension and improves lung growth in infant rats after neonatal treatment with a VEGF receptor inhibitor. Am J Physiol Lung Cell Mol Physiol 2004;287:L344–L351. [PubMed: 15064225]
34. Tell G, Pines A, Paron I, D'Elia A, Bisca A, Kelley MR, Manzini G, Damante G. Redox effector factor-1 regulates the activity of thyroid transcription factor 1 by controlling the redox state of the N transcriptional activation domain. J Biol Chem 2002;277:14564–14574. [PubMed: 11834746]
35. Warner BB, Stuart LA, Papes RA, Wispe JR. Functional and pathological effects of prolonged hyperoxia in neonatal mice. Am J Physiol Lung Cell Mol Physiol 1998;275:L110–L117.
36. Young SL, Evans K, Eu JP. Nitric oxide modulates branching morphogenesis in fetal rat lung explants. Am J Physiol Lung Cell Mol Physiol 2002;282:L379–L385. [PubMed: 11839530]

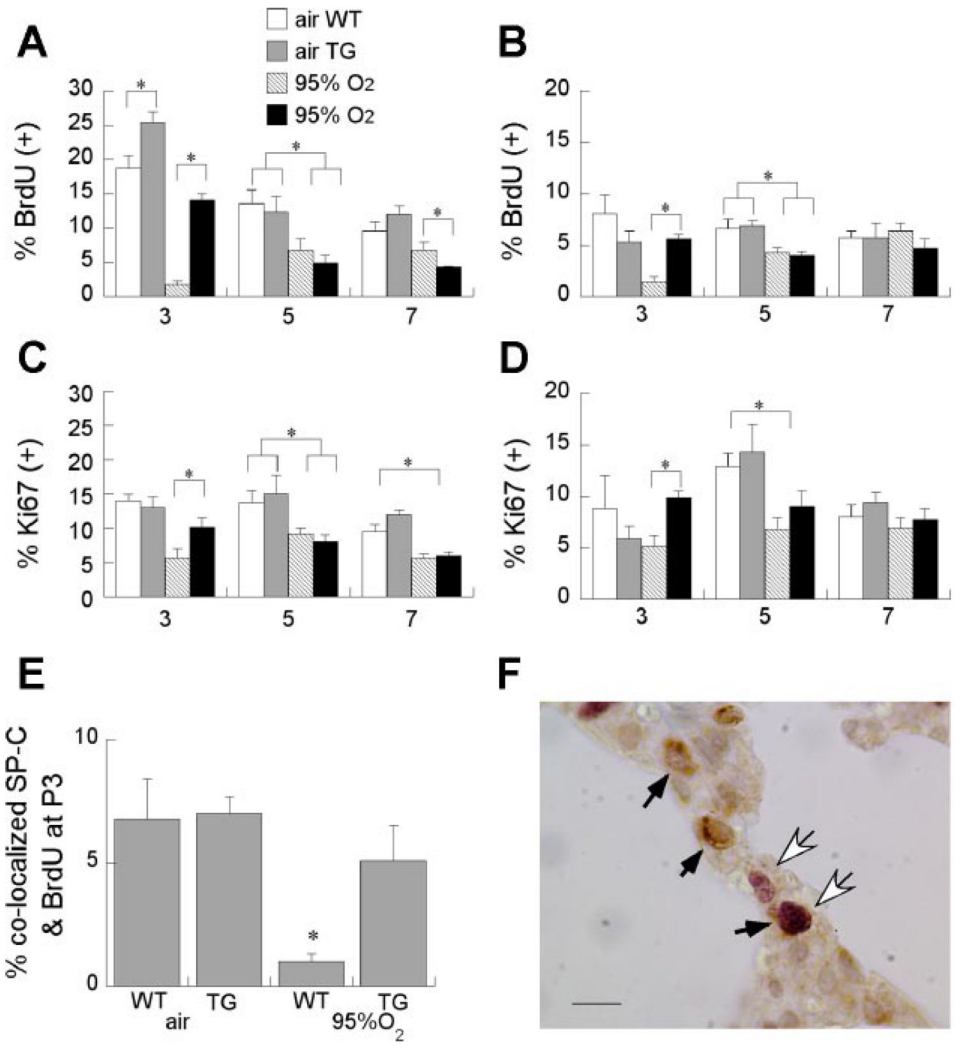

Fig. 1.

Effect of hyperoxia and transgenic (TG) extracellular superoxide dismutase (EC-SOD) on alveolar and bronchiolar epithelial proliferation at postnatal *days 3*, *5*, and *7* (P3, P5, and P7). Bromodeoxyuridine (BrdU) labeling indexes in cells lining distal air sacs (*A*) or bronchioles (*B*); means are 6 pups/group + SE. **P* < 0.05 for indicated comparisons. Ki67 labeling indexes for cells lining air sacs (*C*) or bronchioles (*D*). *E*: BrdU labeling indexes for type II [surfactant protein C (SP-C)-positive cells], 5 pups/group, means + SE. **P* < 0.05 wild type (WT) vs. TG. *F*: SP-C-immunostained (brown) cells are shown by black arrows; BrdU-labeled (purple) cells are shown by white arrows.

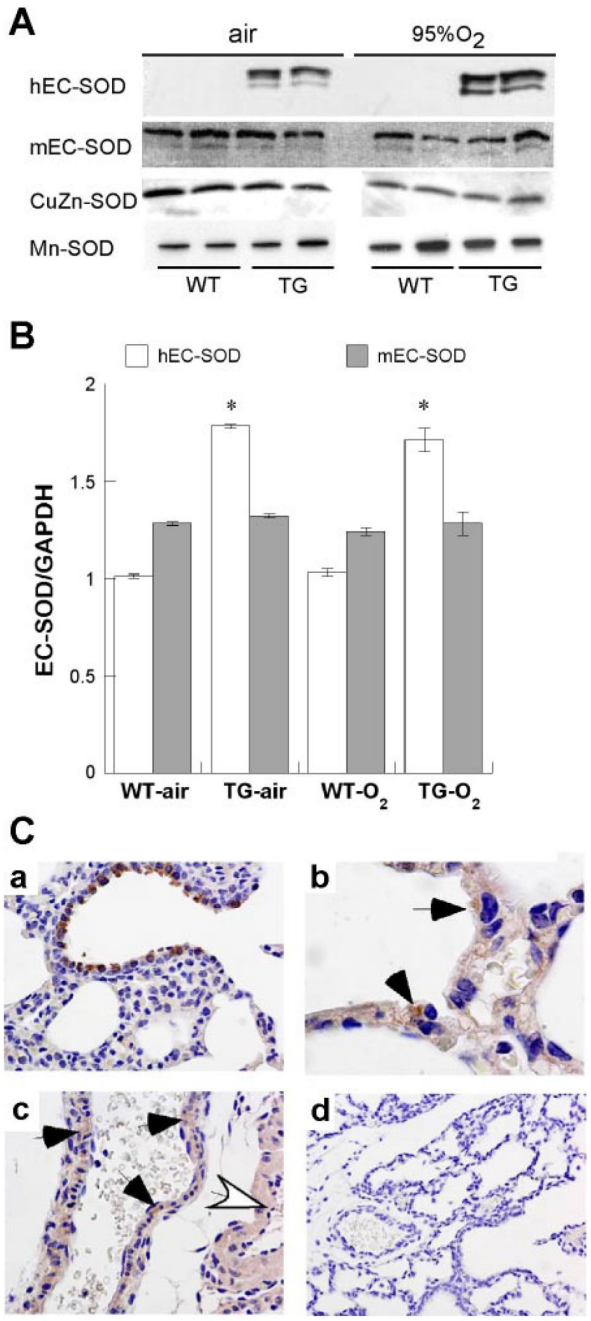

Fig. 2.

Effect of hyperoxia and TG EC-SOD on mouse (m) and human (h) EC-SOD expression. *A*: representative immunoblots detecting human and mouse EC-SOD, CuZn-SOD, and Mn-SOD. *B*: mean hEC-SOD or mEC-SOD mRNA real-time PCR signals at crossing point of amplification, normalized to glyceraldehyde-3-phosphate dehydrogenase (GAPDH) signal + SE, 8 pups/condition. *$P < 0.05$ vs. WT. *C*: mEC-SOD expression (*A*), airway, ×200; alveolar epithelium (*B*), arrows, ×1,000; and vascular smooth muscle (*C*) in small artery (black arrows) and large artery (white arrow), ×200. *D* shows control with no primary antibody, ×200.

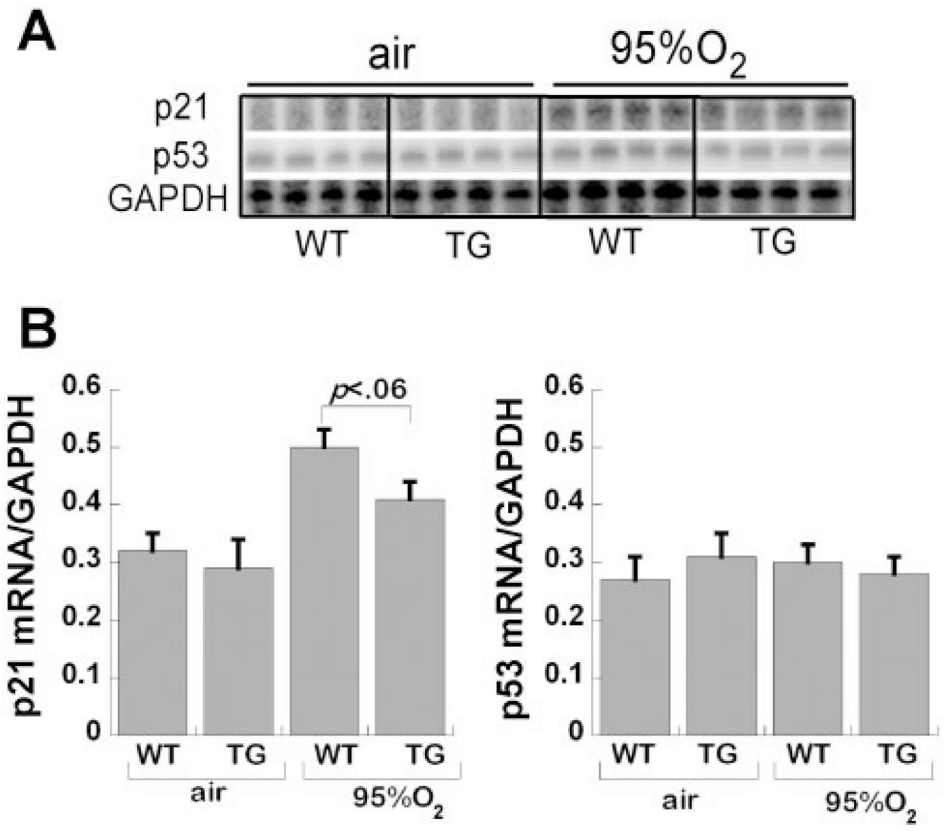

Fig. 3.

Effect of hyperoxia and TG EC-SOD on p21$^{cip/waf}$ and p53 expression. *A*: RNase protection assay autofluorogram detecting p21, p53, and GAPDH mRNA in air- and 95% O_2-exposed animals, WT and TG, quantified in graph. *B*: values are pixels for p21 or p53, each normalized to corresponding GAPDH signal in each lane, mean of 8 pups/group + SE.

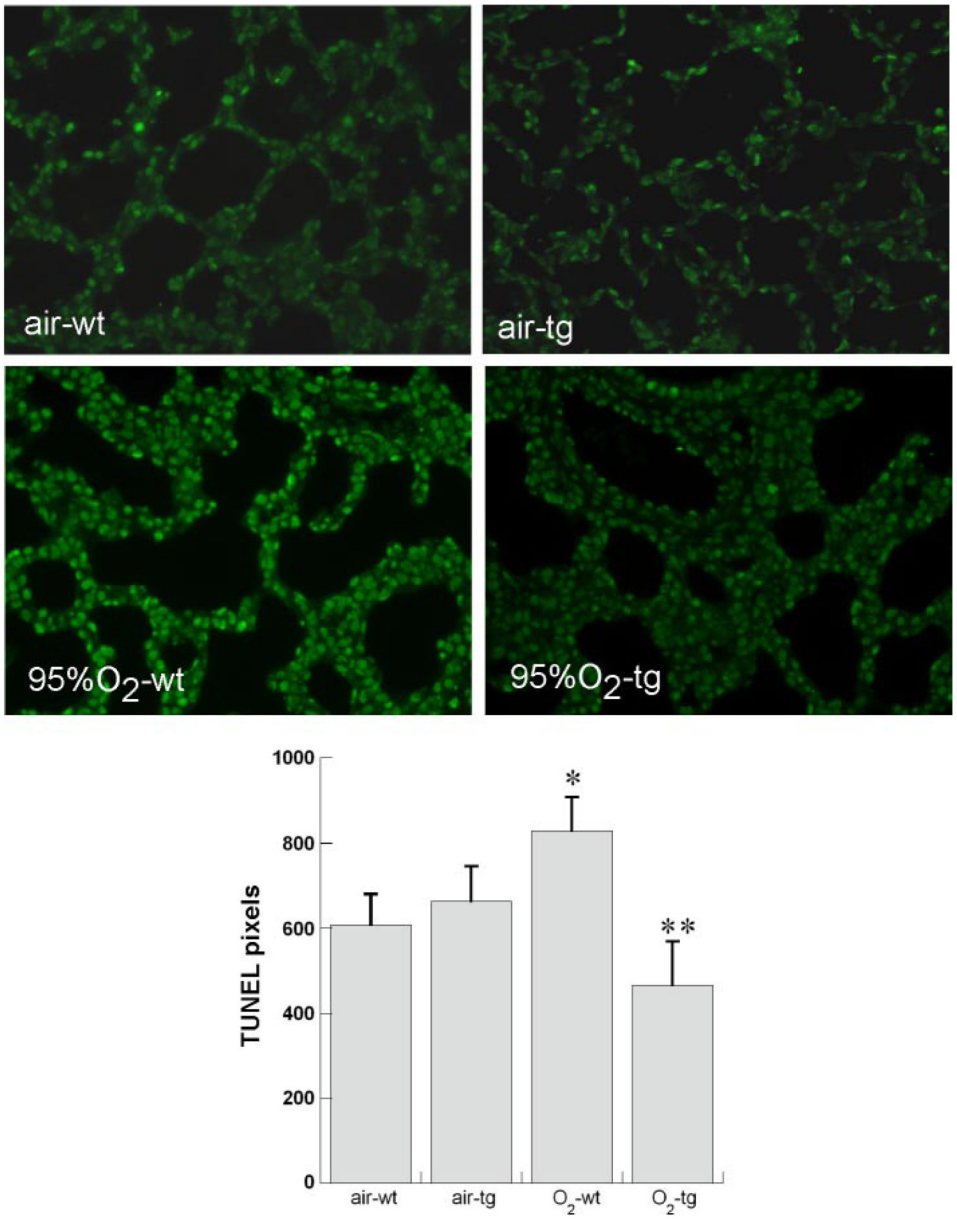

Fig. 4.

Effect of hyperoxia and TG EC-SOD on DNA nicking [TdT-mediated dUTP nick end labeling (TUNEL)] at P3. *Top*: representative photomicrographs (×200 magnification) for each condition. *Bottom*: mean TUNEL intensity in pixels normalized to nuclear area (4′,6-diamidino-2-phenylindole perimeter), 5 pups/group + SE. **P* < 0.05 vs. air WT, ***P* < 0.05 vs. O_2 WT.

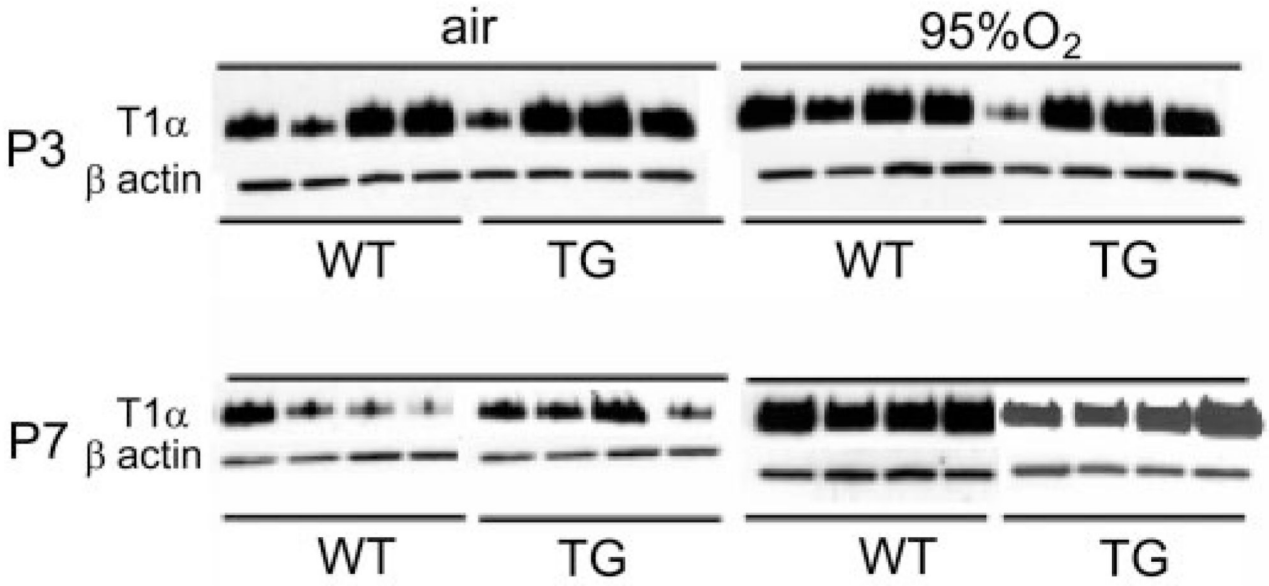

Fig. 5.

Effect of hyperoxia and TG EC-SOD on type I cell α protein (T1α) shown by Western blot. Effect of air, 95% O_2, and TG EC-SOD on T1α and β-actin in whole lung homogenates at P3 and P7.

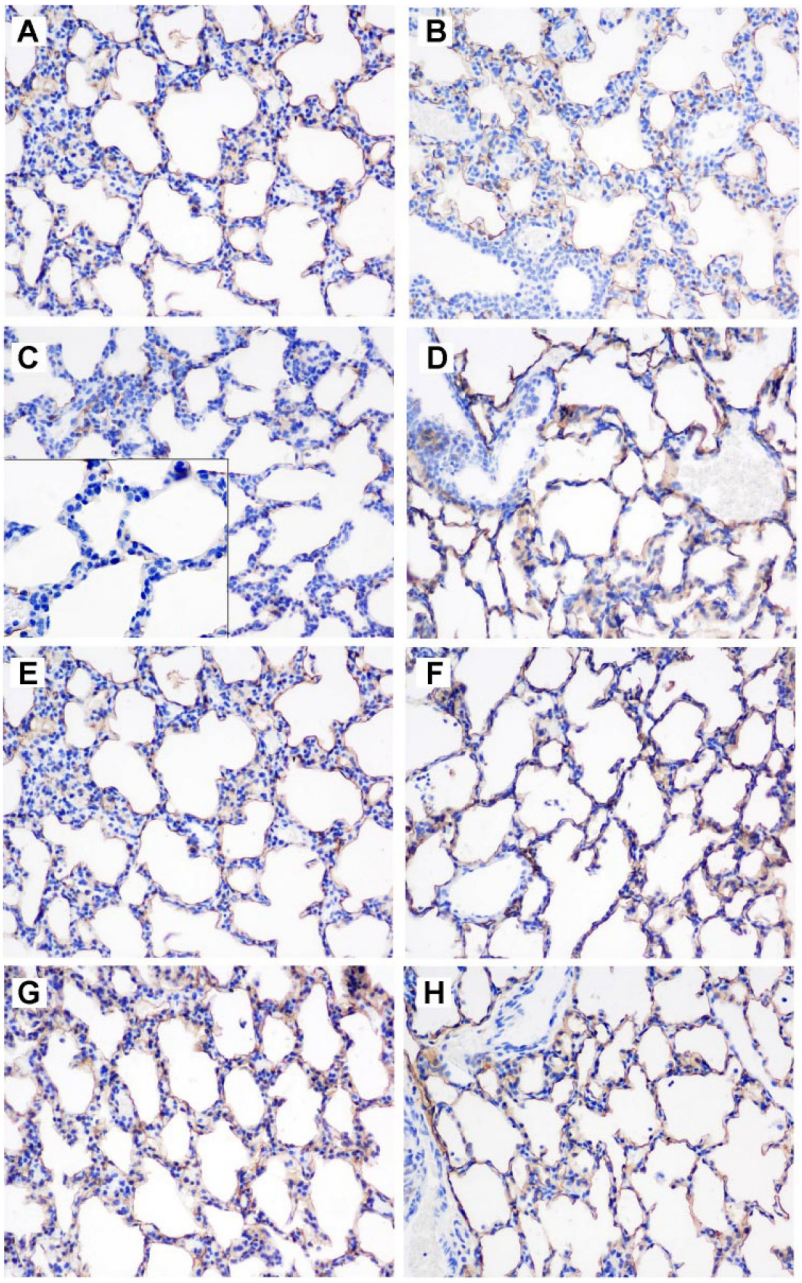

Fig. 6.

Effect of hyperoxia and TG EC-SOD on T1α shown by immunohistochemistry. T1α expression at P3 (*A–D*) in air (*A*, WT; *B*, TG) and 95% O_2-exposed mice (*C*, WT; *D*, TG) and P7 (*E–H*) in air (*E*, WT; *F*, TG) and 95% O_2-exposed mice (*G*, WT; *H*, TG); final magnification, ×200. *C*, *inset*: magnification at ×400 shows lack of apical T1α staining in 95% O_2-exposed WT mice at P3.